RSC Advances

COMMUNICATION

Optical and photodetector properties of stripe-like InS crystal†

Ching-Hwa Ho,*[a] Ya-Han Chen[a] and Jhih-Hao Ho[b]

Cite this: *RSC Adv.*, 2016, **6**, 97445

Received 12th September 2016
Accepted 4th October 2016

DOI: 10.1039/c6ra22743k

www.rsc.org/advances

Stripe-like InS crystals have been grown by physical vapor transport method. Transmission electron microscopy, scanning electron microscopy, optical microscope and Raman measurement characterize the outline shape and orthorhombic structure of the as-grown InS. A prototype photo-metal-semiconductor-field-effect transistor (Photo-MESFET) has been made by a stripe and layer-like InS crystal with Ag for the drain and source contacts and Au for the gate metal. Transmittance results determine its band gap, and the value of about 1.78 eV renders InS more sensitive to near infrared (NIR) than to visible-light optical response. V_{SD}–I_{SD} measurements show p-channel conduction behavior of the InS Photo-MESFET. Under the illumination of a tungsten lamp of power density ~3 mW cm^{-2}, the transconductance gain reaches $g_m = 0.272 \pm 0.005$ μA V^{-1}.

1. Introduction

Starting from the enthusiastic study of graphene, 2D layered semiconductors have demonstrated great promise for implementation of next generation planar and flexible devices. The advantage of using 2D semiconductors is the ultrathin thickness that can be obtained from van der Waals separation of layers, which reveals atomic flatness with decreasing dangling bonds and reducing surface roughness, therefore enhancing the carrier mobility of electrical transport. Nowadays there are mainly two groups of layered-type chalcogenides of most interest: transition-metal dichalcogenides (TMDCs) used for integrated electronics (*e.g.* MoS_2 (ref. 1 and 2)) and III–VI compounds available for optical and electrical device application (*e.g.* GaSe[3] and InSe[4,5]). For the III–VI chalcogenides, because of the misvalency of the compounds (*i.e.* dissimilar to the III–V group, which has a matched valence-electron number) they often show a variety of valency-changed structures with different stoichiometry and crystalline phases in the crystals (*e.g.* In_2Se_3, Ga_2S_3, In_6S_7, and ε-, β- and γ-GaSe).[6–8] Especially InS has been rarely studied, and research and reported information are insufficient to show its device properties and performance.

InS compound has been claimed to possess two different crystalline phases (network and metastable layer) constructed by the connection of a fundamental S–In–In–S unit.[9] The most stabilized phase is the orthorhombic structure with connection in network form, *i.e.* $a = 3.944$, $b = 4.447$, and $c = 10.648$ Å.[10–12] The c plane is a general layered plane of the InS. However, the study of the properties and a prototype device of a new material are beneficial to its further development. In this communication, we characterize the structural properties of orthorhombic InS by high resolution transmission electron microscopy (HRTEM) and polarization-dependent Raman measurement. The experimental band edge was characterized by transmittance measurement. A prototype of InS micro-stripe Photo-MESFET has been firstly fabricated and its device performance is evaluated.

2. Experiments

The layer and stripe-like InS crystals were grown by physical vapor transport (PVT) method using a temperature setting of 750 → 690 °C with a gradient of −3 °C cm^{-1} inside an evacuated and sealed quartz ampoule. The detailed experimental procedure for the PVT growth is described elsewhere.[5] The difference between PVT and chemical vapor transport (CVT) growth is the absence of transport agent (*e.g.* I_2 and ICl_3). For Raman measurement, a RAMaker micro-Raman spectrometer equipped with a 532 nm solid-state laser was used. The laser spot size was reduced to 5 μm and the power was adjusted to about 5 mW. The polarized Raman experiment was done with linearly polarized laser light parallel and perpendicular to the InS crystal's a axis. Transmittance measurement was carried out in a monochromator system, where a 150 W tungsten halogen lamp filtered by a PTI 0.2 m monochromator provides the

[a]Graduate Institute of Applied Science and Technology, National Taiwan University of Science and Technology, Taipei 106, Taiwan. E-mail: chho@mail.ntust.edu.tw; Fax: +886 2 27303733; Tel: +886 2 27303772

[b]Department of Chemistry, National Central University, Zhong-Li, Taoyuan 320, Taiwan

† Electronic supplementary information (ESI) available. See DOI: 10.1039/c6ra22743k

monochromatic light. Bulk photoconductivity measurement was implemented in a stripe-like InS crystal. A white-light LED and a tungsten halogen lamp acted as the white-light sources. For the I_{SD}–V_{SD} test of the Photo-MESFET (*i.e.* the sample thickness is ~0.5 μm on mica), the voltage scanning range of a semiconductor parameter analyzer was set at −40 to 40 V and the tungsten halogen lamp acted as the white light emulator with power density set at ~3 mW cm^{-2} *via* the monitor of an OPHIR optical power meter. A microprobe station facilitated the experiments.

3. Results and discussion

Fig. 1(a) shows the polarization-dependent Raman spectra of an InS micro stripe with unpolarized (lower), $Z(XX)\bar{Z}$ (middle), and $Z(XY)\bar{Z}$ (upper) polarizations. The crystal morphology of the stripe-like InS is also displayed in the microscope-image inset of Fig. 1(a). The crystal orientations of the micro-stripe InS are defined as $a = x$, $b = y$, and $c = z$. The InS crystallizes in an orthorhombic layer structure and the a axis is the longest edge of the InS micro stripe (see ESI† for detailed structural characterization of InS). Prior to the analysis of the polarized Raman spectra, the crystal structure of InS will be firstly discussed. Displayed in Fig. 1(b) are the c-plane scanning-electron-microscope (SEM) and HRTEM images of the orthorhombic InS, where the a and b axes are clearly shown to have orthogonality. Energy dispersive X-ray analysis of the InS using SEM and HRTEM revealed that the stoichiometric ratio of the indium sulfide is In : S = 1 : 1 within a standard error of ±3%. The representative scheme of atomic arrangement of the c-plane InS is shown in Fig. 1(b) as an indication. The gray circles represent In atoms and the yellow circles mark sulfur sites. Essentially the c plane was formed by many top layer In–S bond units arranged horizontally and vertically along the a and b axes. The angle between the a and b axes is 90°, which reveals the orthogonal and orthorhombic structure of the InS. From the estimate of lattice spacing in HRTEM, the lattice constants of the orthorhombic InS are $a \approx 0.4$ nm and $b \approx 0.44$ nm. Fig. S1 in the ESI† also displays this information. The values of lattice constant match well with the reported data of InS.[10,11]

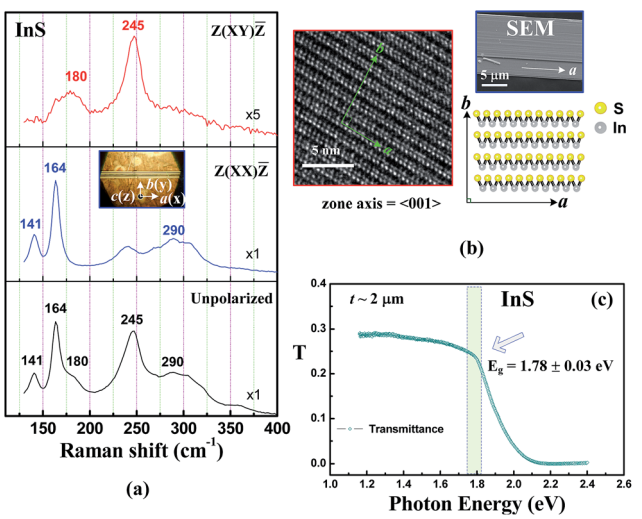

Fig. 1 (a) Polarization-dependent Raman spectra of a PVT-grown InS micro stripe. The inset shows the crystal-morphology image and crystal orientations. (b) SEM and HRTEM images of the c-plane InS. The representative scheme of atomic arrangement in the c plane is also included. (c) Transmittance spectrum of the InS layer for the determination of the energy gap.

As shown in the SEM and HRTEM images as well as the atomic arrangement in Fig. 1(b), the a axis presents the zigzag connection of the indium and sulfur atoms, which displays the longest edge of the InS stripe. The construction of an InS stripe as well as the energy dispersive X-ray (EDX) data can also be evident in Fig. S2 in ESI.† The microscope image shown in Fig. 1(a) also identifies the outline shape of InS as stripe like. The result implies that the structural anisotropy of the a–b axes can occur in the c plane. As shown in the unpolarized Raman spectrum of the c-plane InS in Fig. 1(a), five vibration modes at 141, 164, 180, 245, 290 cm^{-1} can be simultaneously detected. The 141, 161, and 290 cm^{-1} peak modes are enhanced in the $E\|a$-axis polarization with $Z(XX)\bar{Z}$ configuration, while the 180 and 245 cm^{-1} peaks are dominant in the $Z(XY)\bar{Z}$ spectrum. The Raman selection rule clearly identifies the structural anisotropy of the a and b axes in the c plane of the micro-stripe-like InS. The vibration modes along $Z(XX)\bar{Z}$ polarization consist of In–In and S–S relative atomic movements in a zigzag chain connection along the a axis while the $Z(XY)\bar{Z}$ related modes may possess the In–S mutual displacements in the c plane. To further characterize the band gap of the InS, transmittance measurement of an InS layer crystal (thickness ~ 2 μm) was implemented. Fig. 1(c) shows the transmittance spectrum of InS between 1.2 and 2.4 eV. It is clearly shown that the absorption edge of the transmittance spectrum is about 1.7–2.0 eV. The transmission measurement of Fig. 1(c) indicates that ~30% of light can pass through the InS layer in the energy range of 1.2 to 1.5 eV. The energy portion of the knee spectrum closely relates to the band gap of InS. From the estimate in Fig. 1(c), the band gap of InS can be determined to be about 1.78 ± 0.03 eV, close to the NIR to red-light portion.[13] The band value gap also matches well with the crystal color of InS shown in Fig. S2(a).† The valence band top of the InS may consist of S $3p_x$ and $3p_y$ with optical polarization dependence.[14] The polarized behavior of Raman measurement also verified the a–b axes' structural anisotropy, as the results show in Fig. 1(a) and (b).

To evaluate the optoelectronics and electric performance of InS, a stripe-like InS photoconductor (bulk, size ~2 × 0.4 × 0.03 mm) patterned with Ag as the ohmic-contact electrodes was implemented. The lower inset in Fig. 2(a) depicts the representative scheme of the InS photoconductor together with the photo V–I measurement configuration of the photoconductor. The light sources for the photo V–I measurement are a white-light LED and a tungsten halogen (W) lamp with a controlled power density $P \sim 5.5$ mW cm^{-2}. As shown in Fig. 2(b), the LED covers two hump peaks centered at ~2.81 eV and ~2.26 eV in the visible range and the halogen lamp has a black-body radiation peak at ~1.8 eV. Also shown in Fig. 2(a), each of the photo V–I curves shows ohmic-contact behavior at different illumination conditions. In dark conditions, the resistivity of InS is

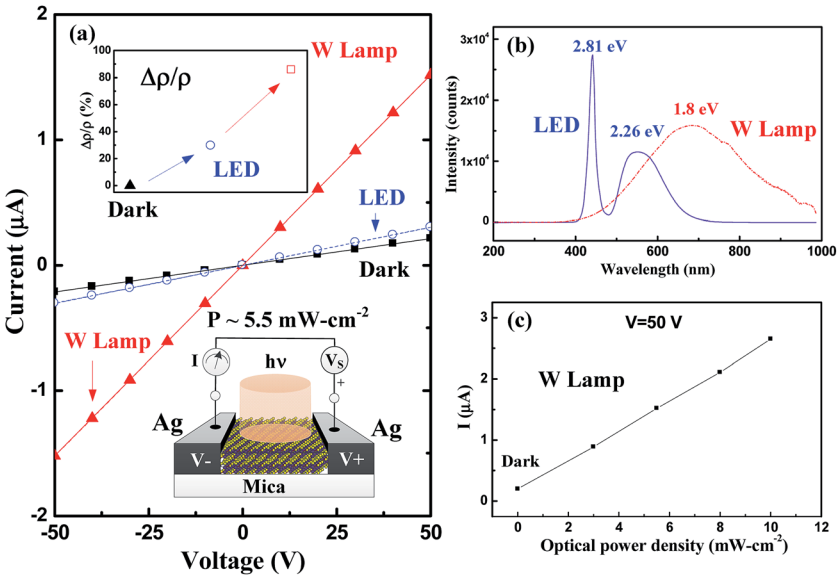

Fig. 2 (a) Photo *V–I* measurement results of bulk InS photoconductor under illumination by different light sources. The lower inset depicts the measurement configuration of the photo *V–I* experiment and upper inset displays the photo-resistivity change ratio ($\Delta\rho/\rho$) under different illumination conditions. (b) Emission spectra of the LED and W lamp white-light sources. (c) Photocurrent change of the bulk InS photoconductor under different optical power densities of W lamp illuminations.

about 1.54×10^5 Ω cm, much larger than the previously reported 10^{-2} to 3 Ω cm of other InS crystals.[15] The result indicates high purity (low impurity concentration) of the as-grown 2D stripe- and layer-like InS crystals. Hall and resistivity measurements of the InS also reveal p-type semiconductor behavior with the carrier concentration $p \sim 1 \times 10^{12}$ cm^{-3} and Hall mobility $\mu \sim 41$ cm^2 V^{-1} s^{-1} at room temperature. The value of Hall mobility is comparable with the drift mobility of ~40 cm^2 V^{-1} s^{-1} that was calculated from the dark resistivity in Fig. 2(a). As shown in Fig. 2(a), the photo *V–I* results show that the photoconductive response by W lamp is higher than that of the other white LED owing to the band gap of InS (~1.78 eV) being near the peak response of the tungsten lamp. The photo-resistivity ratio $\Delta\rho/\rho_{dark}$ of InS under the illumination of a W lamp at 5.5 mW cm^{-2} is ~86%. Fig. 2(c) demonstrates the photocurrent response of the InS stripe photoconductor under different optical power densities of the W lamp from 0 to 10 mW cm^{-2}. The applied voltage is 50 V. As the power increased, the photocurrent enlarged linearly. At $P = 10$ mW cm^{-2}, the current of the InS photoconductor reaches about 2.65 μA. Besides, our previous photoresponsivity spectrum and lower-energy thermoreflectance spectrum of the stripe-like InS also indicated that an intermediate band (IB) and an acceptor level (by defects) may co-exist in the indirect gap of the III–VI InS defect semiconductor (not showing here). The defect band in InS could be the auxiliary of photoelectric transition and conduction in the NIR absorption of the monosulfide.

Fig. 3(a) shows the V_{SD}–I_{SD} measurement results of an InS micro-stripe Photo-MESFET made by an InS layer type photoconductor (*i.e.* size ~ 15 × 40 × 0.5 μm on mica) under the illumination of a W lamp with power density ~3 mW cm^{-2}. The inset shows the measurement-circuit configuration of the Photo-MESFET. The Schottky contact of the metal gate was made of Au for the phototransistor (*i.e.* gate reversed leakage is below 150 nA). As shown in Fig. 3(a), the source–drain voltage scanning range (V_{SD}) is from −40 V to +40 V operated at different gate voltages (V_G) of −20 V to 20 V. It is clear that the I_{SD} values in the V_G range of −20 to −2 V show much larger current than those of $V_G = 2$ to 20 V when $V_{SD} > 0$ V. The result indicates the Photo-MESFET is exactly a p-channel device coming from a p-type semiconductor. It also sustains the Hall measurement result of the InS. The p-type conduction behavior of the Photo-MESFET also implies the existence of an acceptor level in the indirect band gap of InS. As shown in Fig. 3(a), each I_{SD}–V_{SD} curve of different V_G bias also shows a different cut-off voltage along the V_{SD} axis. It signifies that scanning V_{SD} will alter the threshold voltage from the gate terminal in the InS Photo-MESFET. Fig. 3(b) depicts I_{SD} *vs.* V_G under different V_{SD} values from 14 to 28 V for the analysis of transconductance (g_m) of the InS Photo-MESFET. Essentially, the I_{SD} *vs.* V_G curves show linear and parallel dependence to the Photo-MESFET. The photo transconductance can be obtained from the slope fit of the InS Photo-MESFET in Fig. 3(b), and the value is determined to be $g_m = |\partial I_{SD}/\partial V_G|_{V_{SD}} = 0.272 \pm 0.005$ μA V^{-1} under the illumination of a W lamp with a power density of ~3 mW cm^{-2} [*i.e.* the dark current is $I_{SD} \approx 80$ nA with $V_G = 0$ V and $V_{SD} = 40$ V in Fig. 3(a)]. The transconductance g_m of InS Photo-MESFET of 0.272 ± 0.005 μA V^{-1} (by W lamp of $P \approx 3$ mW cm^{-2}, $E_g = 1.78$ eV) shows lower than that of the other III–VI layered InSe Photo-MESFET of $(3.09 \pm 0.22) \times 10^2$ μA V^{-1} (by W lamp at $P \approx 0.5$ mW cm^{-2}, $E_g = 1.25$ eV)[16] due to the direct band gap character (high absorption efficiency) of the layered InSe. The spectral photoresponsivity of InSe is about 7.3 A W^{-1} and is 3–4 A W^{-1} for InS (facilitated by IB) at 1.25 eV.[16] However, the InS phototransistor would be the first prototype optoelectronics device for further application of stripe-like orthorhombic indium monosulfide.

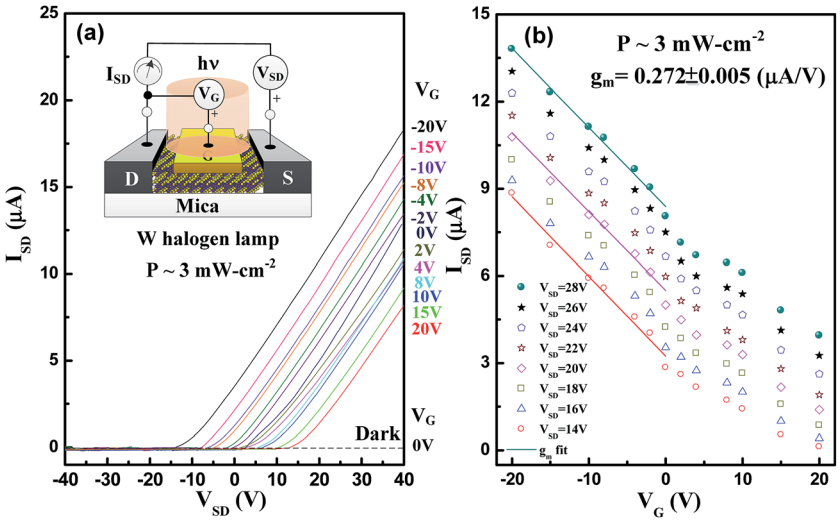

Fig. 3 (a) The I_{SD}–V_{SD} curves of an InS microstripe Photo-MESFET at different gate biases under the illumination of a tungsten halogen lamp of power density $P \sim 3$ mW cm^{-2}. The I–V curve of the dark condition is shown by a dashed curve. (b) The analysis of I_{SD} *vs.* V_G at different V_{SD} for the determination of transconductance g_m in the InS Photo-MESFET.

4. Conclusions

In conclusion, single crystals of InS micro stripe were successfully grown by PVT method. HRTEM, SEM and OM images verified that they are stripe- and layer-like crystals with the longest crystal edge along the *a* axis. Polarized Raman measurements show in-plane anisotropy along $Z(XX)\bar{Z}$ and $Z(XY)\bar{Z}$ polarizations for the *a* and *b* axes in the *c*-plane InS. The indirect band gap of the InS is about 1.78 eV at 300 K. Photo *V*–*I* measurement of the InS crystal show a photo-resistivity ratio $\Delta\rho/\rho_{dark} \sim 86\%$ under the illumination of a W lamp at 5.5 mW cm^{-2}. The band-gap value and defect character of the InS may result in a higher response in the NIR region by tungsten lamp than that by LED illumination. A p-channel InS Photo-MESFET was also firstly made based on an InS micro stripe photoconductor of thickness ~0.5 μm. A g_m value of 0.272 ± 0.005 μA V^{-1} could be obtained from the prototype phototransistor under the illumination of a W lamp with a power density of ~3 mW cm^{-2}. It shows a prototype device for InS opto-electronic applications.

Acknowledgements

We would like to acknowledge the financial support from the Ministry of Science and Technology, Taiwan under the grant No. MOST 104-2112-M-011-002-MY3.

Notes and references

1 R. K. Jana and G. L. Snider, *IEEE Electron Device Lett.*, 2016, **37**, 341–344.
2 C.-H. Lee, N. Vardy and W. S. Wong, *IEEE Electron Device Lett.*, 2016, **37**, 731–734.
3 K. Liu, J. Xu and X. C. Zhang, *Appl. Phys. Lett.*, 2004, **85**, 863–865.
4 S. Sucharitakul, N. J. Goble, U. R. Kumar, R. Sankar, Z. A. Bogorad, F. C. Chou, Y. T. Chen and X. P. A. Gao, *Nano Lett.*, 2015, **15**, 3815–3819.
5 C. H. Ho and Y. J. Chu, *Adv. Opt. Mater.*, 2015, **3**, 1750–1758.
6 J. Zhou, Q. Zeng, D. Lv, L. Sun, L. Niu, W. Fei, F. Liu, Z. Shen, C. Jin and Z. Liu, *Nano Lett.*, 2015, **15**, 6400–6405.
7 H. F. Liu, K. K. A. Antwi, N. L. Yakovlev, H. R. Tan, L. T. Ong, S. J. Chua and D. Z. Chi, *ACS Appl. Mater. Interfaces*, 2014, **6**, 3501–3507.
8 C. H. Ho, Y. P. Wang and Y. S. Huang, *Appl. Phys. Lett.*, 2012, **100**, 131905.
9 J. A. Hollingsworth, D. M. Poojary, A. Clearfield and W. E. Buhro, *J. Am. Chem. Soc.*, 2000, **122**, 3562–3563.
10 W. J. Duffin and J. H. C. Hogg, *Acta Crystallogr.*, 1966, **20**, 566–569.
11 A. Datta, S. Gorai, S. K. Panda and S. Chaudhuri, *Cryst. Growth Des.*, 2006, **6**, 1010–1013.
12 P. Kushwaha, A. Patra, E. Anjali, H. Surdi, A. Singh, C. Gurada, S. Ramakrishnan, S. S. Prabhu, A. V. Gopal and A. Thamizhavel, *Opt. Mater.*, 2014, **36**, 616–620.
13 M. A. M. Seyam, *Vacuum*, 2001, **63**, 441–447.
14 K. Takarabe and T. Nishino, *J. Phys. Chem. Solids*, 1983, **44**, 681–684.
15 T. Nishino and Y. Hamakawa, *Jpn. J. Appl. Phys.*, 1977, **16**, 1291–1300.
16 C. H. Ho, *2D Mater.*, 2016, **3**, 025019.

Electronic Supplementary Material (ESI) for RSC Advances.

Supporting Information

Optical and Photodetector Properties of Stripe-Like InS Crystal

Ching-Hwa Ho[a,*] Ya-Han Chen,[a] and Jhih-Hao Ho[b]

[a] Graduate Institute of Applied Science and Technology, National Taiwan University of Science and Technology, Taipei 106, Taiwan

[b] Department of Chemistry, National Central University, Zhong-Li, Taoyuan 320, Taiwan

[*]E-mail: chho@mail.ntust.edu.tw

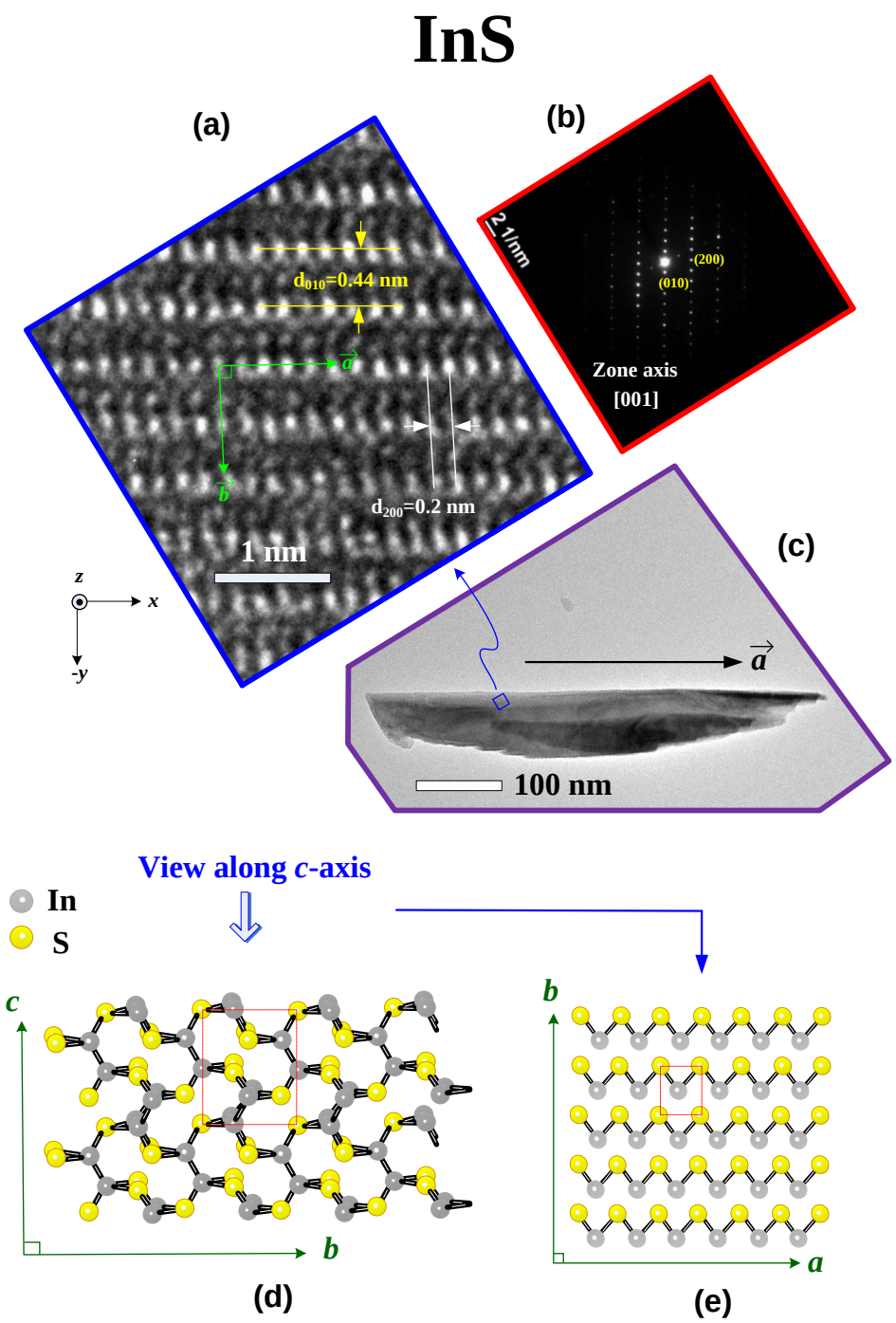

Fig. S1. (a) HRTEM image and (b) SAED pattern of a stripe-like nanoflake in (c) for a *c*-plane InS grown by physical vapor transport method. An orthorhombic lattice is clearly shown and the longest edge of the plate is along *a* axis. (d) The representative scheme of atomic arrangement in network form of orthorhombic InS. (e) The atomic sites and HRTEM image of the stripe-like InS viewing along *c* axis. The atomic arrangements show similar pattern, and which is consisted of fundamental In-S bond units that constructed and connected orthogonally.

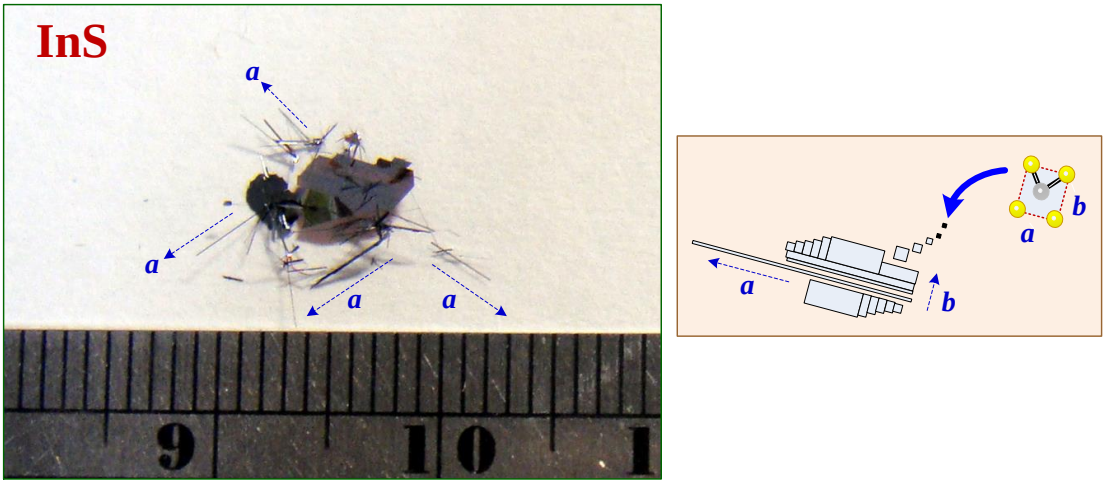

(a)

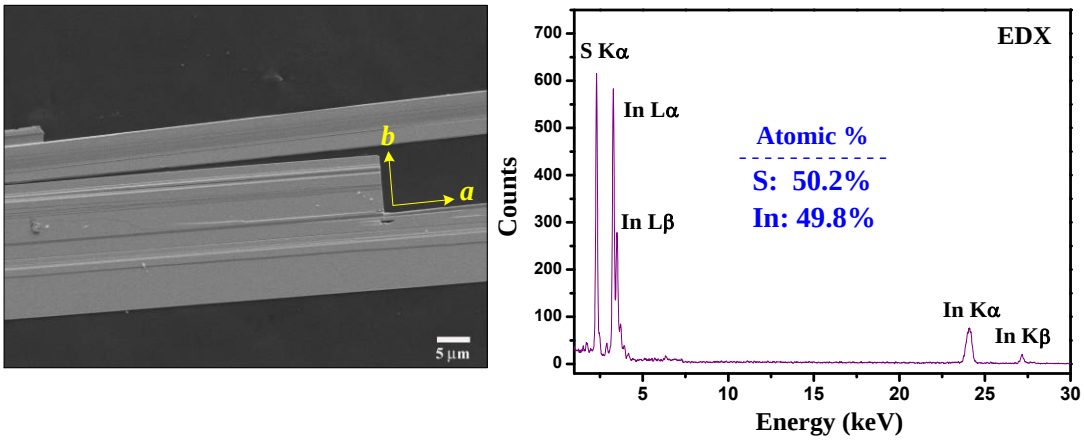

(b)

Fig. S2. (a) Crystal morphology of the as-grown InS that includes needle, stripe, and layer like outline. The needle and stripe like InS crystals are extension along *a* axis. The large-area layer shows dark red and transparent to verify its band-edge energy. The right inset depicts the construction of nano needle, stripe, ribbon and layered orthorhombic InS from fundamental In-S bond units. (b) SEM image and EDX result of the InS microstripes. They verify orthogonality and stoichiometry of the as-grown InS nano (micro) stripes.

Figures S1(a) and 1(b) respectively show the HRTEM image as well as selective-area-electron-diffraction (SAED) pattern in a stripe-like nanoribbon displayed in Fig. S1(c) grown by PVT. The zone axis of the electron beam of the TEM images is along <001>. The clear atomic sites in Fig. S1(a) as well as obvious dot pattern in SAED image in Fig. 1(b) indicate high crystalline quality of the as-grown InS nanoflake. As shown in Fig. S1(a), the angle between *a* and *b* axes (green lines) are 90°, which reveals orthogonal and orthorhombic structure of the InS. The lattice spacing in Fig. 1(a) verifies that the lattice constants of orthorhombic InS are $a \approx 0.4$ nm (i.e. $d_{200}=0.2$ nm) and $b \approx 0.44$ nm, respectively. The *a* axis consists of the connection of zigzag chain of indium-sulfur atoms, which is the longest edge of the InS nanoribbon as displayed in Fig. S1(c). The great ionic character (ionicity) of InS that relative to the other InSe, GaS and GaSe monochalcogenides may destabilize the usual hexagonal-layer structure and becomes a network-connection structure in the orthorhombic InS.[17] The atomic arrangement of the lowest-energy network form (i.e. high-temperature phase) [9] of the S-In-In-S units with sharing corner style in InS is depicted in Fig. S1(d). A sharing-corner connection to the fundamental S-In-In-S units instead of van der Waals gap of the hexagonal layer stacking, represents for the network form of the orthorhombic InS along *c* axis. The *c* plane (*a*-*b* surface) viewed along *c* axis is depicted in Fig. S1(e). Essentially the *c* plane was formed by many top

layer In-S zigzag bond units that arranged horizontally and vertically along the *a* and *b* axes.

To further understand crystallographic construction of the network InS, larger and long-range-order as-grown crystals are prepared and their crystal morphologies are displayed in the left part in Fig. S2(a). The outline shapes of the InS reveal needle, stripe, and layer-like styles that may consist of small to a larger-area crystal construction. Especially, the larger area and layer like InS shows dark red and transparent, which can be evident in Fig. S2(a). The result indicates the band gap of the InS crystal is near red-light wavelength portion.[13] The thin-plate type morphology of InS also identifies a 2D layer-like character of the monosulfide. The right part in Fig. S2(a) shows the representative scheme of building in orthorhombic InS from the basic In-S bond unit as derived in Fig. S1(e). Initially, the nearly square-shape In-S units (i.e. $a \approx 0.4$ nm and $b \approx 0.44$ nm) can be connected or merged together along either *a*-, *b*- or both axes to form a needle, stripe, rectangular, square-like, or polygon *c*-plane as indicated in the right side of Fig. S2(a). The binding force along *a* axis (zigzag chain) is larger than that along *b* axis, which can be verified from many of as-grown stripe and ribbon-like InS crystals were formed alongside *a* axis in Fig. S2(a). The various widths of small stripe-like InS crystals are ranged from ~tens nm to tens μm. The stripe-like outline and orthorhombic structure of the network InS can

also be observed and verified by scanning electron microscope (SEM) image of InS as displayed in Fig. S2(b). The axial direction of the *c*-plane micro- and nano- stripes is along *a* axis, which may be the strongest bonding-force orientation of the InS. The angle between *a* and *b* axes is 90°. The right part in Fig. S2(b) shows the energy-dispersive X-ray (EDX) spectrum of the as-grown InS, which shows approximately 1:1 (In:S) stoichiometric content for the InS micro- and nano-stripe. The network InS structure has an orthorhombic lattice with a crystal symmetry of space group D_{2h}^{12}.[18, 19]

Supporting Information Reference:

17 K. Takarabe, K. Wakamura, and T. Ogawa, *J. Phys. Soc. Jpn.* 1983, **52**, 686-693.

18 N. M. Gasanly, N. F. Gakhramanov, B. M. Dzhavadov, V. I. Tagirov, and E. A. Vinogradov, *Phys. Stat. Sol. (b)* 1979, **95**, K89-K92.

19 F. E. Faradzhev, N. M. Gasanly, A. S. Ragimov, A. F. Goncharov, and S. I. Subbotin, *Solid State Commun.* 1981, **39**, 587-589.